Steady Flow in an Aneurysm Model: Correlation Between Fluid Dynamics and Blood Platelet Deposition

D. Bluestein

L. Niu

R. T. Schoephoerster

Mechanical Engineering Department,
Florida International University,
Miami, FL 33199

M. K. Dewanjee

Department of Radiology,
Division of Nuclear Medicine,
University of Miami,
Miami, FL 33136

Laminar and turbulent numerical simulations of steady flow in an aneurysm model were carried out over Reynolds numbers ranging from 300 to 3600. The numerical simulations are validated with Digital Particle Image Velocimetry (DPIV) measurements, and used to study the fluid dynamic mechanisms that characterize aneurysm deterioration, by correlating them to in vitro blood platelet deposition results. It is shown that the recirculation zone formed inside the aneurysm cavity creates conditions that promote thrombus formation and the viability of rupture. Wall shear stress values in the recirculation zone are around one order of magnitude less than in the entrance zone. The point of reattachment at the distal end of the aneurysm is characterized by a pronounced wall shear stress peak. As the Reynolds number increases in laminar flow, the center of the recirculation region migrates toward the distal end of the aneurysm, increasing the pressure at the reattachment point. Under fully turbulent flow conditions (Re = 3600) the recirculation zone inside the aneurysm shrinks considerably. The wall shear stress values are almost one order of magnitude larger than those for the laminar cases. The fluid dynamics mechanisms inferred from the numerical simulation were correlated with measurements of blood platelet deposition, offering useful explanations for the different morphologies of the platelet deposition curves.

Introduction

Abdominal aortic aneurysms (AAA) are among the most lethal clinical phenomena among people 55 years of age or older. Post mortem autopsies reveal that they occur in about 2 percent of the population, while aneurysms of all kinds are seen in up to 10 percent of all postmortem examinations (Johansen, 1982). An aneurysm is defined as a focal dilatation of a blood vessel involving an increase in diameter above 50 percent compared with the expected normal diameter. Aneurysms that are not treated to elective aneurysmectomy surgery, involving an aortic resection and reconstruction with a dacron graft, may rupture eventually. Up to 62 percent of the patients with ruptured aneurysms die before reaching the hospital. When these prehospital deaths are counted, the overall mortality rate may exceed 90 percent (Ingoldby et al., 1986, Thomas and Stewart, 1988). The increasing median age of the population contributes to an increasing incidence (Ernst, 1993).

An aneurysm may occur when the arterial wall loses its structural integrity and gives way to the distending force of the pulsatile intraluminal pressure. A segment of the artery expands to form a balloon-like dilatation: an aneurysm. Once initiated, the tension on its wall increases obeying Laplace's law that states that the tension in the wall is directly proportional to the product of the intraluminal pressure and the radius of the dilatation. As the thickness of the wall must play a role in the distension and ultimate rupture of an aneurysm, the stress in the arterial wall was shown to be also inversely proportional to the wall thickness (Johansen, 1982). As the volume of the arterial wall presumably remains constant, the wall thickness must decrease as the aneurysm enlarges, resulting in rapidly increasing tensile stress. It is important to note that increasing age is accompanied by a reduction of the elasticity of the vessel wall. As the aneurysm progresses, the stiffening of the arterial wall predisposes it to rupture.

As the aneurysm develops, its wall becomes lined with a mural thrombus: an aggregate of blood cells, platelets, blood protein and cellular debris. The thrombus grows as material is deposited from the flowing blood and protrudes into the lumen. Besides rupture, other complications arises as bits of mural thrombus may break off and be carried downstream; these emboli can be lodged in a smaller blood vessel and interrupt the flow of blood. The growing mural thrombus may also occlude blood flow through the aneurysm. It has been argued that the thrombus represents an attempt of the body to increase the wall thickness, thereby reducing the likelihood of rupture, but the gelatinous mass can only be marginally helpful in resisting rupture. Aneurysms in smaller arteries supplying the head and extremities have a lower risk of rupturing than those of the aorta, but have a greater risk of thrombosis and embolization (Johansen, 1982).

Abdominal aortic aneurysms have usually been characterized as atherosclerotic, although no unified concept of pathogenesis has emerged (Ernst, 1993). The genesis of blood coagulation is a cascade phenomena of biochemical events induced by several clotting factors. Transfer of platelets and other clotting factors to the vascular wall is accomplished through diffusive and convective mechanisms. Predilection sites of thrombosis in the human arterial system include geometries which produce nonparallel streamline flow such as bifurcations, branches, curves, stenoses, and aneurysms. Convection of flow aggregates can be locally enhanced or diminished in such geometries that produce localized regions of high and low shear, flow separation, recirculation, and reattachment.

The process of thrombosis may be affected by a series of rheological and fluid dynamic parameters. Based on in vivo

Contributed by the Bioengineering Division for publication in the JOURNAL OF BIOMECHANICAL ENGINEERING. Manuscript received by the Bioengineering Division September 20, 1994; revised manuscript received June 14, 1995. Associate Technical Editor: J. M. Tarbell.

experiments, Fry (1968) concluded that high shear stresses caused injury to the endothelial lining, initiating atherosclerosis. Changes in mass transfer coefficients in regions of relatively low wall shear stress were shown to be responsible for the localization of atherosclerosis (Caro et al., 1971). High rates of shear, areas of flow stagnation or recirculation, and turbulence, were shown to promote thrombus formation (Karino et al., 1987, Folie and McIntire, 1989). Studies of the carotid artery (Ku et al., 1985) and the abdominal aorta (Friedman et al., 1981, Friedman et al., 1992) have found that low mean and oscillating wall shear stresses correlate with atherosclerotic plaque localization. Near wall excesses of platelets in tube flow have been reported (Eckstein and Belgacem, 1991, Tangelder et al., 1982, Aarts et al., 1988, Schoephoerster et al., 1993) to be dependent, among other factors, on flow conditions (wall shear rate, tube diameter). Stein and Sabbah (1974) have correlated turbulence with thrombus formation on artificial surfaces. Actual deposition of platelets onto artificial surfaces tends to increase with increasing shear due to increased collision frequency and mass transfer (Christenson et al., 1981, Lelah et al., 1984). Direct correlations of local fluid dynamic events with platelet aggregation in vortices and adhesion onto surfaces were obtained in low Reynolds number flow through an abrupt expansion (Karino and Goldsmith, 1979a and 1979b). The degree to which these mechanisms play a role in the pathogenesis of AAA is still under question (Dobrin, 1989), though the above mentioned studies clearly indicate that the coexistence of both high shear stress zone and low shear stress or recirculating zone promote thrombus formation.

There are several aneurysm hemodynamics in vitro studies in steady flow (Scherer, 1973, Drexler and Hoffman, 1985, Budwig et al., 1993). These studies have shown that the flow field through the aneurysm is characterized by a jet of fluid surrounded by a recirculating vortex. A typical value of the Reynolds number in a healthy human abdominal aorta is approximately 1800 during peak systole, but this value can dramatically change as a result of various pathologies. Thus in vitro studies comprise a range of Reynolds numbers anywhere between a few hundreds to a few thousands. Scherer found that the flow through the aneurysm was turbulent when the Reynolds number (based on the bulge diameter) was greater than 2900. Budwig et al. (1993) found that the recirculating vortex effects dramatically the stresses on the aneurysm wall, with wall shear stresses in the recirculation zone dropping to about ten times less than in the entrance tube. The shear stress profile was characterized by two peaks near the reattachment point at the distal end of the aneurysm. Turbulence in the aneurysm was intermittent for $2000 < \mathrm{Re} < 2500$, with a turbulent slug amplified considerably in intensity and length as it went through the aneurysm. These in vitro findings conform with recent in vivo results of cerebral aneurysms (Steiger, 1990) and AAAs (Bluth et al., 1990) that have shown that the flow is sometimes laminar and sometimes turbulent. Arterial-wall vibrations at low frequencies (up to 200 Hz) that are characteristic of turbulent flow fluctuations, were reported to be highly destructive to structural components of the wall (Johansen, 1982). An insight to the mechanism of thrombus formation in aneurysms was given by Muraki (1983) who performed ultrasonic studies of AAAs and suggested that the mural thrombi in aneurysms is initially formed in the distal area of the expansion and then develops proximally. Muraki also observed that aneurysm rupture typically occurs in the distal area of the aneurysm. Other in vitro studies include numerical studies of pulsatile flow through the aneurysm (Wille, 1981; Perktold, 1987; Fukushima et al., 1989; Taylor and Yamaguchi, 1994). Fukushima presents wall shear stresses and also flow visualization photographs, Wille presents velocity vector, streamline, and pressure field results, Perktold mainly presents path lines, and Taylor and Yamaguchi present three dimensional simulation of an asymmetrical aneurysm. Although recently there is a growing body of literature of both in vitro and in vivo results, studies of flow through aneurysms that correlate clinical hemodynamic parameters, e.g., platelet deposition, to the fluid dynamics through the aneurysm, are almost non-existent. Our group has recently used radioactive tagging of platelets to measure the platelet deposition on the wall in a model aneurysm under steady flow conditions (Schoephoerster et al., 1993). The current study is aimed at correlating these results with numerical results of flow through the same model under similar flow conditions, as to shed light on the fluid dynamic mechanisms that lead to thrombus formation inside the aneurysm and the dilatation of the aneurysm.

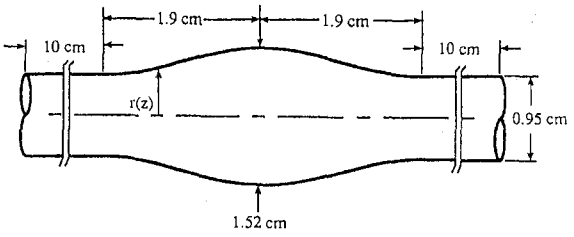

Fig. 1 Geometry of model aneurysm

Methods

Both experimental and numerical methods were used to study steady in vitro flow patterns through a model aneurysm (Fig. 1) under laminar and turbulent flow conditions. The geometry of the model followed the function: $r(z) = 0.47 + 0.14\ \{1 + \cos(\pi z/1.9)\}$, where $r(z)$ is the local radius of the tube and z is measured in cm in the axial direction from the center of the expansion. Numerical modeling of the flow through the aneurysm was conducted using FIDAP (Fluid Dynamics International, Evanston, IL 60201) CFD package. The FIDAP program utilizes a finite element procedure, using the Galerkin form of the Method of Weighted Residuals (Saad et al., 1983), to solve the Navier-Stokes equations:

$$\rho\left(\frac{\partial u_i}{\partial t} + u_j u_{i,j}\right) = \sigma_{ij,i} + \rho f_i \qquad (1)$$

$$\frac{\partial \rho}{\partial t} + (\rho u_j)_j = 0 \qquad (2)$$

where Einstein summation notation was used ($u_i = (u, v, w)$ and a repeated subscript implies summation). The pressure is eliminated from the momentum equations, and solved from the continuity equation (Eq. (2)) by replacing the zero on the right hand side with a very small penalty parameter. The progressive

Nomenclature

AAA = abdominal aortic aneurysm
CFD = computational fluid dynamics
d = diameter
f = body forces
k = turbulent kinetic energy
L = liters
NPD = normalized platelet deposition
r = radial coordinate
Re = Reynolds number
t = time
u = velocity
z = axial coordinate
ϵ = viscous dissipation rate of turbulent kinetic energy
μ = viscosity
ν = dynamic viscosity
ρ = density
σ = stress

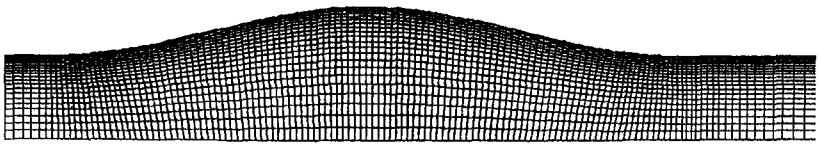

Fig. 2 Typical mesh for finite elements computations in the aneurysm area

density of the finite elements mesh in the radial direction (Fig. 2—the aneurysm area) shows the carefully modelled near wall region. A progressive mesh density in the axial direction was also applied to the inlet region, so that flow conditions at the inlet could be altered from a laminar parabolic velocity profile to a fully developed turbulent velocity profile. The boundary conditions at the inlet were a parabolic velocity profile for the laminar cases, and a plug flow profile that evolved into a fully turbulent velocity profile for the turbulent case. A zero stress zero pressure condition was applied at the outlet, and a no-slip condition was applied at the walls. The entrance lengths were conservatively chosen as 5 diameters for the laminar cases and 8 diameters for the turbulent case, so that the velocity profiles could be fully established proximal to the aneurysm. To find the exit tube length, we examined wall stresses on the aneurysm and the axial velocity profile in the center of the model. Results were independent of exit length for total model length greater than ten diameters. We conservatively selected a model length of 15 diameters. After establishing the numerical results to be independent of mesh density, the mesh consisted of 4000 nine-node quadrilateral elements for the laminar case and 4600 such elements for the turbulent case. In each element biquadratic interpolation functions were used to approximate the velocities. Pressures were approximated using the penalty function approach. The successive substitution method was used for the laminar cases. Simulation of turbulent flow conditions was applied by using the segregated solver method and the standard two equations k-ϵ turbulence model, where the turbulent kinetic energy- k and the viscous dissipation rate of turbulent kinetic energy ϵ, are defined as follows:

$$k = \tfrac{1}{2}\,\overline{u_i' u_i'}, \quad \epsilon = \nu\,\overline{u_{i,j}' u_{i,j}'} \tag{3}$$

In the vicinity of solid boundaries the flow is dominated by viscosity and the use of the k-ϵ model may lead to inferior predictions. FIDAP uses specialized elements for near wall modelling, in which the variation of the turbulent momentum diffusivity is modeled using van Driest's mixing length approach. The combination of the k-ϵ turbulence model with near wall modelling proved to be precise in predicting flow characteristics like reattachment length, as will be discussed later. Axisymmetry was assumed around the longitudinal axis of the aneurysm model, and the blood was assumed to be Newtonian, with real blood properties: $\rho = 1.056$ g/cm^3, $\mu = 3.5$ cPoise, and $\nu = 0.035$ cm^2/s, so that accurate correlations may be made between the fluid simulations and actual blood platelet deposition determined from in vitro experiments.

In order to validate the numerical simulation, quantitative flow visualization was carried out using a Digital Particle Image Velocimetry (DPIV) system (Dantec FlowGrabber™, Dantec Measurement Technology, NJ, USA). The DPIV system is capable of providing a quantitative two-dimensional picture of displacement of particles and the velocity vector field of the flow. The fluid is seeded with particles and single exposure images of the particles illuminated by a laser light sheet are recorded using a video camera and a high speed electronic shutter. The displacements of the particles are obtained by locally cross-correlating sequential images, and the velocity vector fields are computed from the known shutter speed. The cross-correlation function of the two samples is calculated using FFT techniques. The displacement of the cross-correlation peak gives the average spatial shift of the particles in each subsample pair. Details of the method can be found in Willert and Gharib (1991). In order to enhance the DPIV resolution, measurements were carried out in a steady flow loop with a large scale aneurysm model (10:1), following the above mentioned geometry. The model was manufactured from glass and had the following dimensions: inlet diameter-9.8 cm, max. aneurysm diameter-15.68 cm, entry length of 25 diameters, and distal length of 16 diameters. The working fluid was water, seeded with several microns diameter reflective latex beads (Optimage Ltd., Edinburgh, UK) to obtain the velocity vector fields. Dynamic similarity was kept in order to run the DPIV measurements in the respective Re numbers of the numerical simulations.

Platelet deposition results were obtained by radioactive labeling of the blood platelets with In-111, and quantified by measuring the percentage of radioactivity bound to platelets along successive segments of the model aneurysm. The results are given in terms of NPD (Normalized Platelet Deposition), where the local number of platelets per unit area is normalized by the average platelet density over the entire flow chamber. Detailed description of the experimental procedure can be found elsewhere (Schoephoerster et al., 1993).

Results

Numerical Results. Laminar flow results were obtained at three different Reynolds numbers: Re = 300, 900, and 1800 (based on the proximal diameter and the average velocity at the entrance-computed from the corresponding flow rates of 0.5 L/min, 1.5 L/min, and 3 L/min). Turbulent flow results were obtained for Re = 3600 (corresponding to a flow rate of 6 L/min). All the results were characterized by a core flow pattern passing through the center of the aneurysm, surrounded by symmetrical recirculating vortices (Figs. 3(a) through 3(d). For the laminar cases the maximum core flow velocity through the aneurysm (measured at the cross-sections of each corresponding center of recirculation) essentially remained the same as that of the entrance of the tube (Fig. 4), indicating that the central flow through the aneurysm did not bear the nature of a jet flow. Therefore, the main hemodynamic mechanism for thrombus formation in the aneurysm was the slowly recirculating vortex.

For the turbulent case, the maximum core flow velocity through the aneurysm (mean velocity) was 15 percent slower than that of the upstream (Fig. 4). The difference between the laminar and the turbulent cases stems from the fact that the recirculation zone shrunk significantly for the turbulent case, leaving more space for the core flow to expand and slow down. As a result, although the upstream and downstream maximum velocities were approximately 35 percent higher at the centerline for the turbulent case (Re = 3600) as compared to a laminar case (Re = 1800), the maximum velocities through the aneurysm were of similar magnitude for both Reynolds numbers.

The streamline contour plots (Fig. 3(a) through 3(d)) show that as the Reynolds number increased the vortex became skewed, with the center of the recirculation moving downstream, toward the distal end of the aneurysm and closer to the core flow, causing a contraction of the vortex streamlines in the distal edge of the aneurysm and an expansion of the streamlines on the proximal edge. The recirculation zone encompassed a larger area of the aneurysm cavity as the Reynolds number increased.

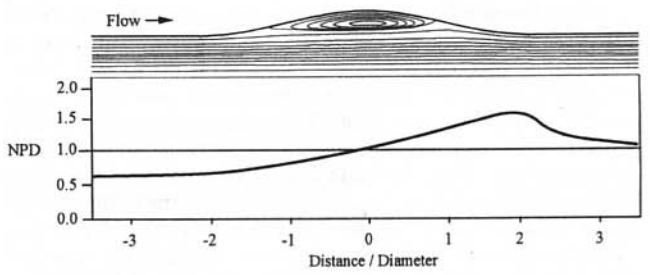

Fig. 3(*a*) Re = 300

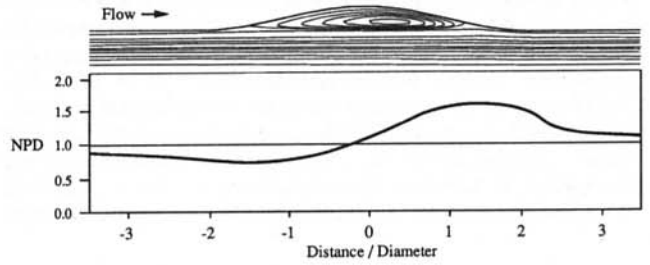

Fig. 3(*b*) Re = 900

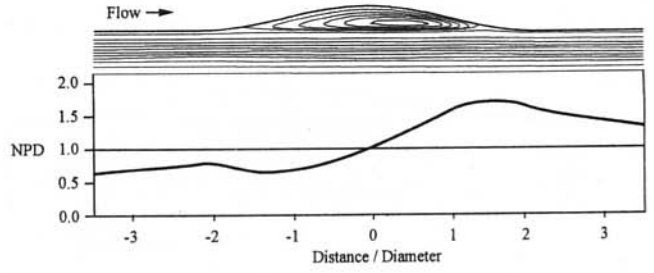

Fig. 3(*c*) Re = 1800

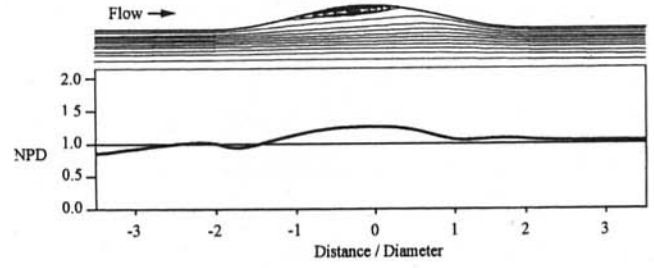

Fig. 3(*d*) Re = 3600

Fig. 3 Streamline contour plots and Normalized Platelet Deposition (NPD) curves at the recirculation zone

A dramatic change occurred when the flow became turbulent (Re = 3600, Fig. 3(*d*). The recirculation zone shrunk considerably; its center of circulation migrating toward the proximal end of the aneurysm. This agrees with results by Young (1979) in a flow through a stenosis. Young showed that the reattachment length in such flows increase with increasing Reynolds number for laminar flow conditions, peaks just before the onset of turbulence, and decreases with increasing Reynolds number when turbulence prevails, eventually reaching a limiting value at high Reynolds numbers. In the case of an aneurysm this mechanism can be explained by the fact that a turbulent velocity profile is more resistant to separation. The delay in separation initiates the recirculation zone deeper inside the aneurysm cavity. The recirculation zone is shortened because it is effectively confined in the proximal side of the aneurysm cavity; the streamlines are already tilted toward the wall of the cavity resulting in a particle path that is bound to reattach earlier to the wall.

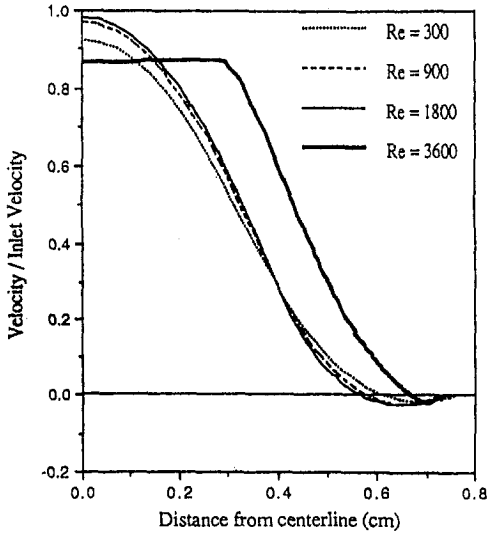

Fig. 4 Velocity profiles at the center of the recirculation zone (normalized with the inlet velocities)

A typical pressure contour plot (Re = 1800) is shown in Fig. 5. The iso-pressure contours show how the pressure reached a minimum at the separation point and increased monotonously along the aneurysm. The pressure peaked at the reattachment point, which constituted a stagnation point, and fell sharply distal to the aneurysm. The pattern of our pressure distribution results agree with those of Taylor and Yamaguchi (1994) for their steady flow case (Re = 700), where the region of maximum pressure occurred at the distal end of the aneurysm. When comparing with their unsteady flow results (peak Re = 1400) when the vortex in the aneurysm is well established (the deceleration phase during late systole), the pattern of our pressure results qualitatively agree with theirs, although it must be cautioned that both separation and reattachment points are in the proximal side for their unsteady flow solution. The pressure distribution results indicate that once an aneurysm is formed, the fluid dynamics inside the cavity will increase the pressure, further dilating the aneurysm. The location of the pressure peak, at the reattachment point, conforms with the findings by Muraki (1983), who observed that aneurysm rupture typically occurs at the distal area.

Wall shear stress results are shown in Fig. 6(*a*), normalized with the wall shear stress at the entrance tube. The wall shear stress declined rapidly to zero around the separation point ($x/d \approx -2$), and maintained a near zero value (negative, because of the flow reversal in the recirculation zone) along the aneurysm. The wall shear stress rose sharply in the reattachment point ($x/d \approx 1.85$) and peaked at $x/d \approx 2$ with a value roughly 1.75 times the upstream value. As the point of reattachment was shared by both the core flow and the recirculating flow, the shear layer created in the interface between the two gradually

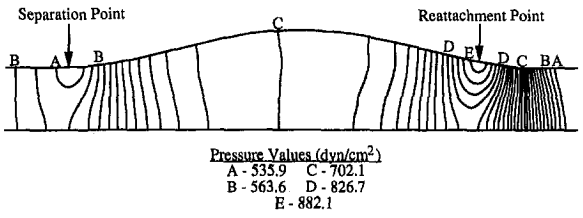

Fig. 5 Typical pressure contour plot (Re = 1800)

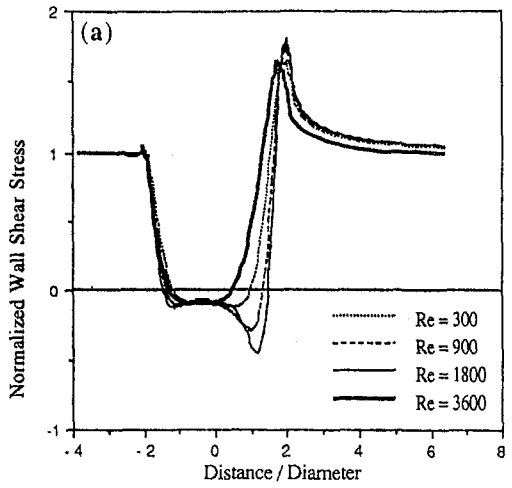

Fig. 6(*a*) Wall shear stress normalized by inlet wall shear stress

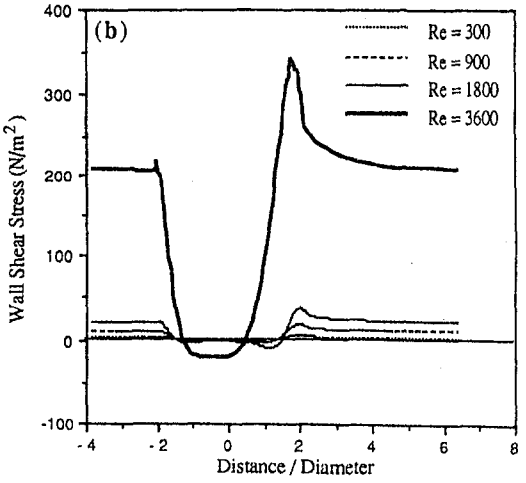

Fig. 6(*b*) Absolute wall shear stress

Fig. 6 Wall shear stress distribution along the aneurysm

decreased the shear stress in the downstream direction, till it approached the upstream value around $x/d = 6$.

The wall shear stress distribution along the aneurysm depicts the main mechanism of platelet deposition along the aneurysm. At the interface between the recirculation and core regions platelets are exposed to elevated shear along the higher velocity side of the shear layer, and at the vicinity of the reattachment point where the wall shear stress peaks. This exposure is relatively prolonged because of the convective deceleration at the interface. These elevated shear histories indicate that platelets approaching the recirculation zone have high incidence of activation. Once trapped in the recirculation zone, the platelets experience low wall shear stresses that allow prolonged contact with the wall, promoting adhesion to the wall.

A closer examination of the absolute wall shear stress values (Fig. 6(*b*)) reveals that for the laminar cases the wall shear stress peaks near the reattachment points increased with increasing Reynolds numbers, corresponding to a spreading out of the platelet deposition peaks, that will be discussed in detail later. The turbulent wall shear stress peak (Re = 3600) migrated upstream, corresponding to the reattachment point of its shrunk recirculation zone. The turbulent wall shear stress values were around one order of magnitude larger than those under laminar flow conditions. The laminar results of the streamlines and wall shear stresses agree with numerical results by Budwig et al. (1993) for $400 \leq Re \leq 2000$, in a similar geometry.

Experimental Validation of the Numerical Results With DPIV. Validation of the numerical simulation results was accomplished by comparing the numerical results to DPIV measurements conducted in an aneurysm model with the same geometry in a steady flow loop. The numerical velocity profiles for Re = 900 were superimposed on a vector plot of the DPIV measurements (Figs. 7(*a*) and 7(*b*)). The superimposed dividing streamline of the recirculation zone according to the numerical simulation was in a good agreement with the DPIV results. A comparison of a characteristic velocity profile in the recirculation zone showed a fairly good agreement, with a slight indication that the measured DPIV velocity profile has not yet reached a fully developed laminar parabolic velocity profile. This could be accounted to the insufficient entry length (25 diameters) for the laminar cases, due to size limitations of our flow loop (441 cm in total length). For the turbulent case (Re = 3600, Fig. 7(*b*)) a very good agreement was achieved between the numerical and DPIV results in predicting a characteristic fully turbulent velocity profile across the aneurysm. This indicates that our assumption of turbulent flow conditions for Re = 3600 was valid, and in agreement with other researchers results (Scherer,

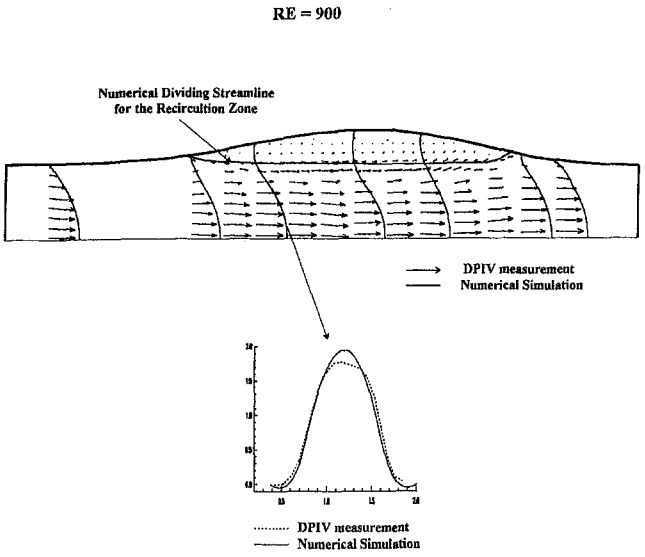

Fig. 7(*a*) Laminar case (Re = 900)

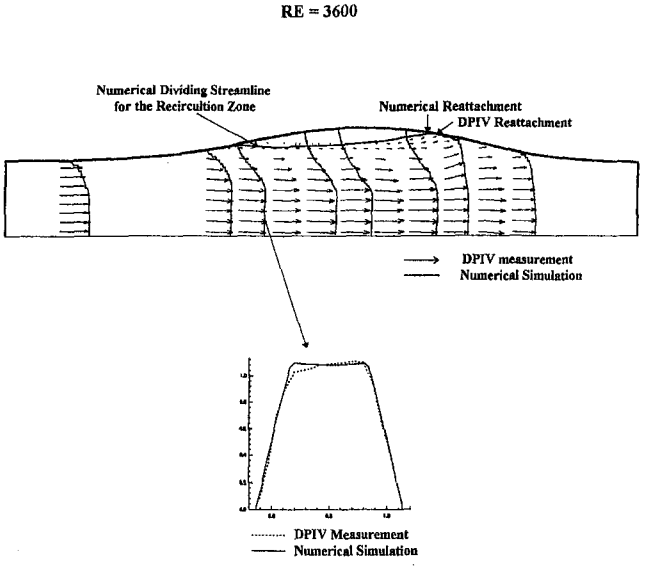

Fig. 7(*b*) Turbulent case (Re = 3600)

Fig. 7 Correlation of numerical results with DPIV measurements

1973, Budwig et al., 1993). The prediction of the separation and reattachment points of the k-ϵ turbulent model was in a fairly good agreement with the DPIV results, with the numerical results predicting a reattachment point slightly upstream from the measured one. This indicates that although our numerical simulation of turbulent flow conditions was carried out in the low Re range, the combination of the k-ϵ turbulent model with specialized elements for near wall modelling, in which the variation of the turbulent momentum diffusivity is modeled using van Driest's mixing length approach, yielded a good prediction of the size of the recirculation zone and the turbulent mean velocities of the flow inside the aneurysm. DPIV measurements of the velocity vectors within the recirculation zone were impaired, partly because of the lack of refractive index matching that produced optical distortion near the wall, and partly because the DPIV could not resolve few of the very low velocities involved. This problem was exacerbated for the turbulent case (Fig. 7(b), Re = 3600), where random fluctuations yielded insufficient correlations to produce meaningful DPIV velocity vectors.

Correlation With Platelet Deposition. In general, under laminar flow conditions an approximately linear increase in NPD was produced in the aneurysm region, increasing in the direction of flow (Fig. 3 a through d). Karino and Goldsmith (1979b) attributed this increase to the enhanced convective transport of platelets and blood cells to the wall along the locally curved streamlines. Streamlines with components perpendicular to the wall will cause the flowing platelets to collide with the wall at higher rates than streamlines parallel to the wall. As the Reynolds number increased, the skewing of the vortex toward the downstream edge of the aneurysm caused a contraction of the streamlines in the distal edge of the aneurysm and an expansion of the streamlines on the proximal edge. As the flow rotated counterclockwise in the vortex region (toward the proximal end of the aneurysm), the number of streamlines carrying platelets within the critical adhesion distance from the wall decreased. As a result, the number of platelets adhering to the wall decreased in the direction of the local flow in the recirculation region, or, from a different frame of reference, increased along the wall of the aneurysm in the direction of the bulk flow.

For flow conditions of Reynolds numbers 300, 900, and 1800 skewed vortex regions were observed, thus creating the approximately linear increases in NPD in the aneurysm in the direction of the bulk flow (Figs. 3(a), (b), and (c)). For the 0.5 L/min flow rate (Re = 300), a very slow moving laminar recirculation zone was confined to the aneurysm, with the dividing streamline almost parallel to the upstream chamber wall. At 1.5 and 3.0 L/min (Re = 900 and 1800, correspondingly), the flow in the annular region of the aneurysm was more disturbed, and the recirculation zone bulged toward the main flow causing the dividing streamline in the main flow to straighten within the aneurysm, inducing disturbances downstream from the aneurysm. This may be causative of the slight increase in NPD distal to the aneurysm compared with the proximal side. With convective transport becoming more dominant as the Reynolds number increased and the vortex being stretched in the direction of flow, the peak NPD became less sharp (more spread out) and the magnitude of the decrease was attenuated. This behavior may be attributed to the combined effect of the stronger convection, manifested through higher wall shear stresses (Fig. 6) that washed away the platelets from the wall, and the stretching of the vortex that decreased the angle of incidence of the dividing streamline along the reattachment point.

As the Reynolds number increased, a small dip in the NPD curves preceded the linear NPD increase. Besides the decrease in the number of streamlines carrying platelets within the critical adhesion distance from the wall in vicinity of the separation point (the proximal end of the aneurysm), the platelets already deposited to the wall at the distal end of the aneurysm generated a deficit in the possible number of recirculating platelets that could adhere to the wall in the proximal region. It should be emphasized here that under steady flow conditions the number of platelets trapped in the recirculation zone remains fairly constant.

At Re = 3600 (Fig. 3(d)), the turbulent fluctuations were effective in disturbing the flow within the aneurysm to the point of dominating the laminar convection mechanisms described above. The linear increase in NPD along the aneurysm was replaced by a lump like NPD distribution curve. As the circulating vortex was much smaller and effectively confined to the proximal side of the cavity, with its center of circulation migrating to the proximal side of the aneurysm, the platelets were more uniformly deposited along the aneurysm. The higher incidence angle of the dividing streamline (point of reattachment) could be accounted for by the gradual decrease of the NPD following the peak. The small dip, similar to those observed in the laminar cases, was proximal to the recirculation zone for the turbulent case, indicating that turbulent fluctuations may have driven away platelets from the wall at the beginning of the aneurysm expansion.

The dynamics of the recirculation vortex for the turbulent case reinforce the notion that the turbulent fluctuations down play the effect of the laminar convection mechanisms. While under laminar flow conditions the platelets are deposited to the wall mainly by locally curved and contracting streamlines, the dominant mechanism under turbulent conditions is the agitated random fluctuations that increases the rate of collisions between platelets. Such collisions serve as an agent for platelet activation, rendering the platelets to adhere to each other, as well as to other surfaces. This mechanism prevails throughout the tube, so that the effect of the diminished recirculation zone in the aneurysm becomes less and less pronounced. Moreover, the steeper velocity gradient near the wall, characteristic of fully turbulent flow conditions, creates higher shear rates that wash away deposited platelets. The overall effect results in a more spread out NPD distribution curve, with less pronounced relative change between the proximal and distal sides.

Conclusions

We have presented results of a numerical simulation of flow through an axisymmetric aneurysm under laminar and turbulent steady flow conditions, and correlated them with experimental blood platelet deposition results obtained in a similar model aneurysm under similar flow conditions. It was shown that the fluid dynamics characterizing the recirculation zone formed inside the aneurysm cavity create conditions that promote thrombus formation and the viability of rupture. Wall shear stresses in the recirculation zone were around one order of magnitude less than in the entrance zone, while the reattachment point at the distal end of the aneurysm created a wall shear stress peak that was roughly twice the entrance shear stress value. The combination of spatially coexisting high and low shear stress zones along the interface of the recirculation zone and the core region, and inside the recirculation zone, promoted thrombus formation inside the aneurysm. Once trapped in the recirculating zone, platelets with elevated shear histories and higher incidence of activation were readily deposited to the wall in areas of low wall shear stress. As the Reynolds number increased, the center of the recirculation region migrated toward the distal end of the aneurysm, subsequently increasing the pressure at the reattachment point. As the flow pattern became fully turbulent, both the recirculation zone inside the aneurysm and the wall shear stress magnitude were altered dramatically. Platelet deposition results correlated with the numerical results. The fluid dynamics mechanisms that could be inferred in details from the numerical simulation, offered useful explanations for the different morphologies of the platelet deposition curves.

The picture that emerges from the combined descriptions of the fluid dynamics and the platelet deposition results agrees

with the in vivo results by Muraki (1983), who examined progressive aneurysms and suggested that the mural thrombi in aneurysms is initially formed in the distal area of the expansion and then develops proximally. While it must be cautioned that these conclusions were drawn from a steady flow simulation, such a simulation fairly approximates late systole pulsatile flow conditions through an aneurysm in terms of the well established recirculation zone that is fairly constant during this period. Nevertheless, future work that will establish similar correlations under pulsatile flow conditions is needed to provide further insight into aneurysm hemodynamics under more realistic conditions.

Acknowledgments

This work was supported in part by grants from the National Institutes of Health (HL46444) and the American Heart Association, Florida Affiliate (9501342).

References

Aarts, P. A., van Den, M. M., Broek, S. A. T., Prins, G. W., Kuiken, D. C., Sixma, J. J., and Heethaar, R. M., 1988, "Blood Platelets Are Concentrated Near the Wall and Red Blood Cells, in the Center in Flowing Blood," *Arteriosclerosis,* Vol. 8, pp. 819–824.

Bluth, E. I., Murphey, S. M., Hollier, L. H., and Sullivan, M. A., 1990, "Color Flow Doppler in the Evaluation of Aortic Aneurysms," *Int. Angio.,* Vol. 9, pp. 8–10.

Budwig, R., Elgar, D., Hooper, H., Slippy, J., 1993, "Steady Flow in Abdominal Aortic Aneurysm Models," *J. Biomed. Engr.,* Vol. 115, pp. 418–423.

Caro, C. G., Fitzgerald, J. M., and Schroter, R. C., 1971, "Atheroma and Wall Shear. Observation, Correlation and Proposal of a Shear Dependent Mass Transfer Mechanism for Atherogenesis." *Proc. Royal Soc. London,* Series B, Vol. 177, pp. 109–159.

Christenson, J. T., Mergerman, J., Hanel, K. C., L'Italien, G. J., Strauss, H. W., and Abbott, W. M., 1981, "The Effect of Blood Flow Rates on Platelet Deposition in PTFE Arterial Bypass Grafts," *Trans. ASAIO,* Vol. 27, pp. 188–191.

Dorbin, P. B., 1989, "Pathophysiology and Pathogenesis of Aortic Aneurysms," *Surg. Clin of N. Amer.,* Vol. 69, pp. 689–703.

Drexler, D. J., and Hoffman, A. H., 1985, "Steady Flow Through Several Aneurysm Models," *Proc. Eleventh Ann. NE Bioengr. Conf.,* W. Kuklinsky and W. Ohley, eds., pp. 147–150.

Eckstein, E. C., and Belgacem, F., 1991, "Model of Platelet Transport in Flowing Blood with Drift and Diffusion Terms," *Biophys. J.,* Vol. 60, pp. 53–69.

Ernst, C. B., 1993, "Abdominal Aortic Aneurysm," *New England J. Med.,* Vol. 328(16), pp. 1167–72.

Folie, B. J., and McIntire, L. V., 1989, "Mathematical Analysis of Mural Thrombogenesis: Concentration Profiles of Platelet-Activating Agents and Effects of Viscous Shear Flow," *Biophysical J.,* Vol. 56(1), pp. 1121–1141.

Friedman, M. H., Hutchins, G. M., and Bargeron, C. B., 1981, "Correlation Between Intimal Thickness and Fluid Shaer in Human Arteries," *Atherosclerosis,* Vol. 39, pp. 425–436.

Friedman, M. H., Bargeron, C. B., Duncan, D. D., Hutchins, G. M., and Mark, F. F., 1992, "Effects of Arterial Compliance and Non-Newtonian Rehology on Correlation Between Intimal Thickness and Wall Shear," ASME JOURNAL OF BIOMECHANICAL ENGINEERING, Vol. 109, pp. 317–320.

Fry, D. L., 1968, "Acute Vascular Endothelial Changes Associated With Increased Blood Velocity Gradients," *Circulation Research,* Vol. 22, pp. 165–197.

Fukushima, T., Matszuzawa, T., and Homma, T., 1986, "Visualization and Finite Element Analysis of Pulsatile Flow in Models of Abdominal Aortic Aneurysm," *Biorehology,* Vol. 26, pp. 109–130.

Ingoldby, C. J. H., Wujanto, R., Mitchell, J. E., 1986, "Impact of Vascular Surgery on Community Mortality From Ruptured Aortic Aneurysms," *Br. J. Surg.,* Vol. 73, pp. 551–3.

Johansen, K. H., 1982, "Aneurysms," *Scientific American,* Vol. 247, pp. 110–125.

Karino, T., and Goldsmith, H. L., 1979a, "Aggregation of Human Platelets in an Annular Vortex Distal to a Tubular Expansion," *Microvasc. Research,* Vol. 17, pp. 217–237.

Karino, T., and Goldsmith, H. L., 1979b, "Adhesion of Human Platelets to Collagen on the Walls Distal to a Tubular Expansion," *Microvasc. Research,* Vol. 17, pp. 238–262.

Karino, T., Goldsmith, H. L., Motomiya, M., Mabuchi, S., and Sohara, Y., 1987, "Flow Patterns in Vessels of Simple and Complex Geometries," *Blood in Contact with Natural and Artificial Surfaces,* Leonard, E. F., Turitto, V. T., and Vroman, L., eds., New York Academy of Sciences, New York, pp. 422–441.

Ku, D. N., Giddens, D. P., Zarins, Z. S., and Glagov, S., 1985, "Pulsatile Flow and Atherosclerosis in Human Carotid Bifurcation," *Atherosclerosis,* Vol. 5, pp. 1047–60.

Lelah, M. D., Lamprecht, L. K., and Cooper, S. L., 1984, "A Canine Ex Vivo Series Shunt for Evaluating Thrombus Deposition on Polymer Surfaces," *J. Biomed. Mater. Res.,* Vol. 18, pp. 475–496.

Muraki, N., 1983, "Ultrasonic Studies of the Abdominal Aorta with Special Reference to Hemodynamic Considerations on Thrombus Formation in the Abdominal Aortic Aneurysm," *J. Japanese College Angiology,* Vol. 23, pp. 401–413.

Perktold, K., 1987, "On the Paths of Fluid Particles in an Axisymmetric Aneurysm," *J. Biomechanics,* Vol. 20, pp. 311–317.

Schoephoerster, R. T., Oynes, F., Nunez, H., Kapadvanjwala, M., and Dewanjee, M. K., 1993, "Effects of Local Geometry and Fluid Dynamics on Regional Platelet Deposition on Artificial Surfaces," *Artherosclerosis and Thrombosis 13,* Vol. 12, pp. 1806–1813.

Steiger, H. J., 1990, "Pathophysiology and Development of Rupture of Cerebral Aneurysms," *Acta Neurchir. Suppl.* (Wien), Vol. 48, pp. 1–57.

Stein, P. D., and Sabbah, H. N., 1974, "Measured Turbulence and its Effect on Thrombus Formation," *Circ. Research.,* Vol. 35, pp. 608–614.

Tangelder, G. J., Slaaf, D. W., Teirlink, H. C., Alewijnse, R., and Reneman, R. S., 1982, "Localization Within a Thin Optical Section of Fluorescent Blood Platelets Flowing in a Microvessel," *Microvasc. Res.,* Vol. 23, pp. 214–230.

Taylor, T. W., and Yamaguchi, T., 1994, "Three Dimensional Simulation of Blood Flow in an Abdominal Aortic Aneurysm-Steady and Unsteady Flow Cases," *J. Biomech. Engr.,* Vol. 116, pp. 89–97.

Thomas, P. R. S., and Stewart, R. D., 1988, *Br. J. Surg.,* Vol. 73, pp. 101–3.

Willert, C. E., and Gharib, M., 1991, "Digital Particle Image Velocimetry," *Experiments in Fluids,* Vol. 10, pp. 181–193.

Wille, S. O., 1981, "Pulsating Pressure and Flow in an Arterial Aneurysm Simulated in a Mathematical Model," *J. Biomed. Engr.,* Vol. 3, pp. 153–158.

Young, D. F., 1979, "Fluid Mechanics of Arterial Stenosis," ASME JOURNAL OF BIOMECHANICAL ENGINEERING, Vol. 101, pp. 101–157.